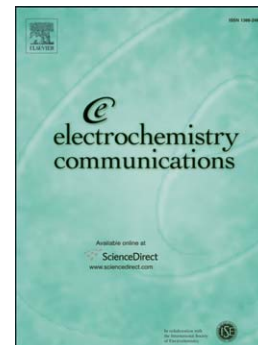# Accepted Manuscript

Characterization of the interfaces between Au(hkl) single crystal basal plane electrodes and [Emmim][Tf$_2$N] ionic liquid

Paula Sebastián, Víctor Climent, Juan M. Feliu

Please cite this article as: Paula Sebastián, Víctor Climent, Juan M. Feliu, Characterization of the interfaces between Au(hkl) single crystal basal plane electrodes and [Emmim][Tf$_2$N] ionic liquid, *Electrochemistry Communications* (2015), doi: 10.1016/j.elecom.2015.11.005

Characterization of the interfaces between Au(hkl) single crystal basal plane electrodes and [Emmim][Tf$_2$N] ionic liquid[*].

Paula Sebastián, Víctor Climent, Juan M. Feliu

Institute of Electrochemistry. University of Alicante. Apdo. 99. 03080 Alicante. Spain

Dedicated to Toni Aldaz

Abstract

The interface between Au(hkl) basal planes and the ionic liquid 1-Ethyl-2,3-dimethyl imidazolium bis(trifluoromethyl)sulfonil imide was investigated by using both cyclic voltammetry and laser-induced temperature jump. Cyclic voltammetry showed characteristic features, revealing surface sensitive processes at the interfaces Au(hkl)/[Emmim][Tf$_2$N]. From laser-induced heating the potential of maximum entropy (pme) is determined. Pme is close to the potential of zero charge (pzc) and, therefore, the technique provides relevant interfacial information. The following order for the pme values has been found: Au(111) > Au(100) > Au(110). This order correlates well with work function data and values of pzc in aqueous solutions.

Introduction

There has recently been considerable interest in the use of room temperature ionic liquids (RTILs) as solvent in a broad range of chemicals applications, including organic synthesis, transition-metal catalyzed reactions, synthesis of macromolecules and nanoparticles, separation processes and spectroscopic measurements[1, 2]. Such applications take advantage of its ability to perform processes that could not be possible in aqueous solutions thanks to its increased thermal stability, particular interaction with some reactants and low vapor pressure. Being composed entirely of ions, RTIL have many electrochemical applications in electrocatalysis, electrodeposition or as solvent in energy devices (batteries and supercapacitors)[3-6].

Despite numerous contributions in the field, the information about the electrochemical interphase between RTILs and well-defined surfaces is scarce. Due to the ionic nature of the RTIL, rationalization of capacitance data using Gouy-Chapman-Stern model is not possible [7] and indirect information techniques are needed [8-20]. The laser temperature jump (LTJ) method has proved valuable in this context. In Au(hkl)/water [21] and Pt(hkl)/water solution [22, 23] interfaces, this experiment supplies the value of the potential of maximum interfacial entropy (pme), which has been shown to be close to the potential of zero charge (pzc). This technique has recently been successfully applied to the Pt(111)/ [Emmim][Tf$_2$N] interface [24].

In this ion-crowded environment, coulombic interactions are certainly the most important in the electrolyte side of the interface. Still, other interaction such as hydrogen bonding between anions and cations must also be considered [25]. In the IL chosen in this study, this latter interaction has been decreased because the hydrogen position in C2 is methylated. Combination of voltammetric and LTJ data performed on well-defined Au(hkl) flame annealed electrodes in contact with purified [Emmim][Tf$_2$N] have been used to characterize these different interfaces. Results are compared with classical data in aqueous solutions.

Experimental

The [Emmim][Tf$_2$N] was purchased from IoLiTec (>99% purity, halides<100ppm, water<60ppm). It was purified following Kolb's procedure [26], namely, dried under vacuum (P<0.002 mbar) more than 24h at 80ºC, followed by treatment with a molecular sieve not larger than 3A. The latter is a key step in the purification process [26-29].

A waveform generator (EG&G PARC 175) together with a potentiostat (eDAQ EA161) and a digital recorder (eDAQ ED401) was employed for cyclic voltammetry experiments. As a quasi-reference electrode, a silver wire was used, but potentials were further referred to Cobaltocenium scale [30]. A Au wire was used as counter electrode. Experiments were carried out with Au(hkl) in the meniscus configuration. A thermostatted cell was used in order to keep the temperature at 25 ºC. Before each

experiment, each Au(hkl) electrode was flame-annealed and cooled down to room temperature under Ar atmosphere.

The LTJ experiment was described elsewhere.[21, 24]. In this experiment, a Nd:YAG pulsed laser is used to cause a sudden change of the temperature of the interphase while the open circuit potential of the working electrode is measured during the temperature relaxation. A system of switches is used to connect / disconnect the potentiostat allowing the polarization of the electrode at the desired potential. In this way, the potentiostat is disconnected just before firing the laser, to ensure true coulostatic conditions. The measured change of the potential contains contributions from the response of the double layer to the temperature change, the spillover of electrons and the thermodiffusion potential. However, it has been demonstrated before [21,24] that the main contribution comes from the effect of the temperature on the polarization of solvent molecules.

Results

Voltammetric experiments

Characteristic voltammetric profiles of Au(100) and Au(110) electrodes in contact with [Emmim][Tf$_2$N] are shown in Figure 1. In both cases, a broad capacitive current signal, which increases linearly with the sweep rate, is superimposed to different couples of sharp peaks. These sharp peaks are similar to those observed during adsorption of organic adlayers on Au(hkl) single crystals corresponding to 2D phase transitions between different ordered structures [31]. Similar sharp peaks are also observed during anion adsorption on Pt(hkl) and Au(hkl) single crystals [32-34]. Interestingly, the characteristic voltammograms are structure sensitive. Starting with Au(110), the most open structure, Figure 1A, three peaks are seen at 1.34, 1.40 and 1.51 V in the positive going sweep. The peaks in the negative going sweep are located at slightly lower potentials, between 10-20 mV less positive than the corresponding anodic counterpart. The interface Au(100)/ [Emmim][Tf$_2$N], figure 1B, features only two couples of peaks, at 1.41 and 1.99 V in the positive-going sweep, with counterparts only 10 mV less positive. The voltammogram is quite stable within this potential range. However, if the upper potential limit is increased, a broad feature starts appearing that modifies the overall profile and both peaks disappear from the voltammogram (Figure 1C). One tentative explanation for this behavior would be that some decomposition product remains adsorbed on the surface. Another possible explanation would be that a reconstruction formed after flame annealing has been lifted during the excursion to high potentials. Additional STM information would be required to discriminate both possibilities.

The most complex voltammetric profile corresponds to Au(111) electrodes (Figure 2A). There are numerous couples of spikes superimposed to two broad capacitive processes that grow below and over 1.7 V, respectively. The reversibility of the peaks is similar to

the previous cases, with a peak to peak separation around 10-20mV. This profile is extremely dependent on the scanned potential window. If the upper potential limit is decreased to 1.6 V (curve a), only a doublet of peaks is observed around 1.44 V. Increasing the upper limit to 2.1 V (curve b) reveals a sharp peak at 2.0 V. Further increasing the upper limit to 2.7 V (curve c), causes the disappearance of the doublet at 1.44 V, with the development of a new couple at 1.34 V and the transformation of the peak at 2.00 V into a new sharper peak at 1.89 V. This peak, centered at 1.89 V, can be used to identify the presence of Au(111) domains in polycrystalline samples. The least quasi-reversible couples at higher potentials (at 2.31 V/2.26 V, and 2.58 V/2.49 V, respectively) do not seem to be affected by the potential scan limit. Cycling the potential in the upper region does not exert further changes in the voltammetric profile. However, if then the potential is cycled again in the low potential region, the peaks at 1.44 (a_1) and 2.0 V (b_1) tend to grow, while those at 1.34 (a_2) and 1.89 V (b_2) tend to decrease. One plausible explanation for this behaviour would be based on the perseverance of the $\sqrt{3}$x22 surface reconstruction at low potential [35]. Peaks a_1 and b_1 would correspond to phase transitions on the reconstructed surface. Then, the excursion to E>2.1 V would cause the lifting of the reconstruction and the appearance of new phase transitions, a_2 and b_2. Negative polarization after lifting of the reconstruction could induce again (partial) reconstruction of the surface and then the recovery of the corresponding phase transitions. An alternative explanation would imply the existence of slow reorganization phenomena in the first cation adlayer in contact with the electrode surface. In this regards, while signals from region c-c' keep unaffected by the sweep rates, the sharp features in regions a-a' and b-b' slightly diminish when the scan rate is decreased but tend to recover their intensity when the sweep rate increases again. This observation could indicate that these peaks do not correspond to true thermodynamic phase transitions, but to metastable situations in which the ionic layer is continuously driven by the potential change.

A question still remaining is the possible effect of impurities in the ionic liquid, especially the small content of water remaining after the purification procedure which could be incorporated into the ionic network. Deliberated additions of water into the IL indicate that this impurity causes a significant increase of the background capacity and the decrease of the sharp spikes reported above (Figure 2B). The presence of small water contents also tend to decrease the potential window before solvent decomposition and that causes the disappearance of the most positive sharp spikes. This experiment demonstrates that water content under the present conditions is lower than 100 ppm and that water is not at the origin of the particular voltammetric behaviour observed here. Still, we cannot rule out completely the participation of water at the interface [36].

An additional experiment was performed to check the existence of irreversibly adsorbed species, that could be formed either from the decomposition of the components of the IL or from impurities that might be present in it. For this purpose, the voltammetric profile of the Au(111) electrode in 0.5 M sulphuric acid solution was recorded after the voltammogram in the ionic liquid. After the experiment in the IL and before introducing

the electrode in the cell with the aqueous solution the electrode was just sonicated for a few minutes in pure water to remove the drop of IL, but not flame annealing was performed to preserve the structure of the surface as was emersed from the IL. Figure 2C shows the comparison of this voltammogram with the one obtained after the usual flame annealing treatment. The profiles are essentially identical, indicating that no irreversibly adsorbed species are formed in the IL. In particular, the sharp spike due to the sulphate disorder/order phase transition is unaffected, demonstrating that the surface remains clean and well-ordered under the presence of the IL.

Laser pulse heating experiments

Figure 3A shows the results of laser pulse heating experiments for Au(111). It is clearly seen that transients change from negative to positive when potential is increased. Similar results are obtained for the other basal planes. When the measurements at different potentials are performed continuously, without annealing in between, a hysteresis is observed between both direction scans. This behavior was previously observed for Pt(111) and attributed to the slow exchange of the cation by the anion in the ionic layered structure [11, 37]. However, the hysteresis for Au is much lower than in the case of Pt(111)[24]. This would agree with the expected lower adsorption strength of the [Emmim][Tf$_2$N] components at gold electrodes.

To overcome these difficulties, to obtain the results reported in figure 3, the electrode was annealed after each measurement at each potential. After annealing, the electrode was contacted with the IL at the desired potential and potential was scanned at 100 mV/s in a narrow potential range to ensure the reproducibility of the voltammetric profile. The potential were the laser induced transient reverses sign has been marked with an arrow in figure 3B, together with the voltammetric profiles corresponding to broader potential window. It can be seen that the highest pme corresponds to Au(111), the lowest being that of Au(110), in good agreement with pzc's in aqueous solution or work function measurements[38]. As it can be seen in Figure 3B, in all cases the pme is located between the onset of cation reduction and the characteristic voltammetric features described above. Therefore, those features are more likely related to interfacial processes where anion presence closer to the electrode is clearly dominant.

Conclusions

The use of purified [Emmim][Tf$_2$N] has revealed unexpected structure sensitivity processes for the three Au(hkl) basal plane electrodes. Among different underlying behavior holding most of the capacitive charge, characteristic sharp spikes have been identified. In the case of Au(111) the surface appears to be quite dynamic and strongly dependent of the potential window used. Since such a voltammetric behaviour reported in the present work have not been reported previously for other IL, we conclude that the chemical nature of the triply methylated cation is at the origin of the surface sensitive voltammetric features.

Laser heating experiments enable to determine the pme values of the three interfaces. The most positive one is that of Au(111)/ [Emmim][Tf$_2$N] and the most negative one corresponds to Au(110)/ [Emmim][Tf$_2$N], in good agreement with pzc values in water solution. It appears that this transient temperature technique supplies significant information of the fundamental properties of Au(hkl)/IL interfaces. More work is in progress to advance in the study of this fundamental subject.
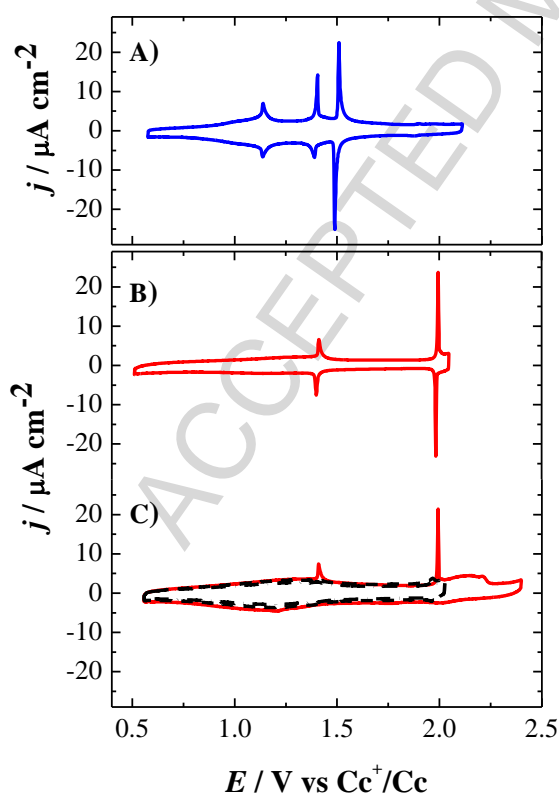
Acknowledgements:

Figure 1: Cyclic voltammograms for A) Au(110) and B) Au(100) in [Emmim][Tf$_2$N]. C): For Au(100), effect of the increase of the upper potential limit up to 2.40 V. Scan rate 50mV s^{-1}.
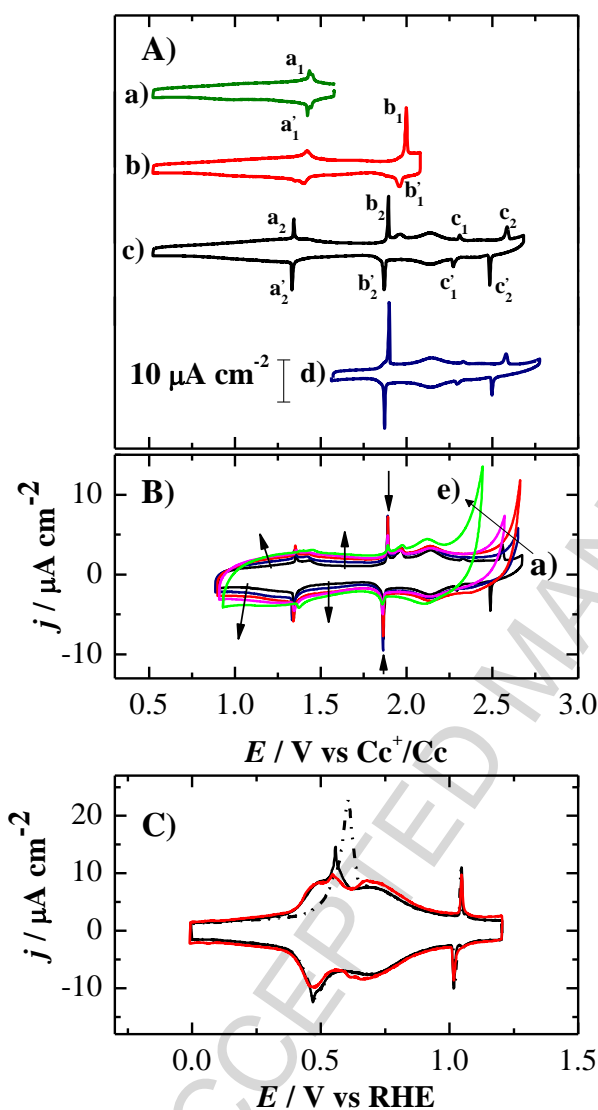
Figure 2: Cyclic voltammograms for: A) Au(111)/[Emmim][Tf$_2$N], different potential limits; B) Au(111)/[Emmim][Tf$_2$N] after adding small amounts of water: a) 0 ppm b) 56.5 ppm , c) 112.5 ppm, d) 544.3 ppm and e) 3125 ppm; C) flame annealed Au(111) / 0.5M H$_2$SO$_4$ first (black dashed line) and second (black solid line) cycle, and after cycling the electrode in the IL (red solid line). Scan rate: 50 mVs^{-1}. Arrows in B) indicate the increase of water content.
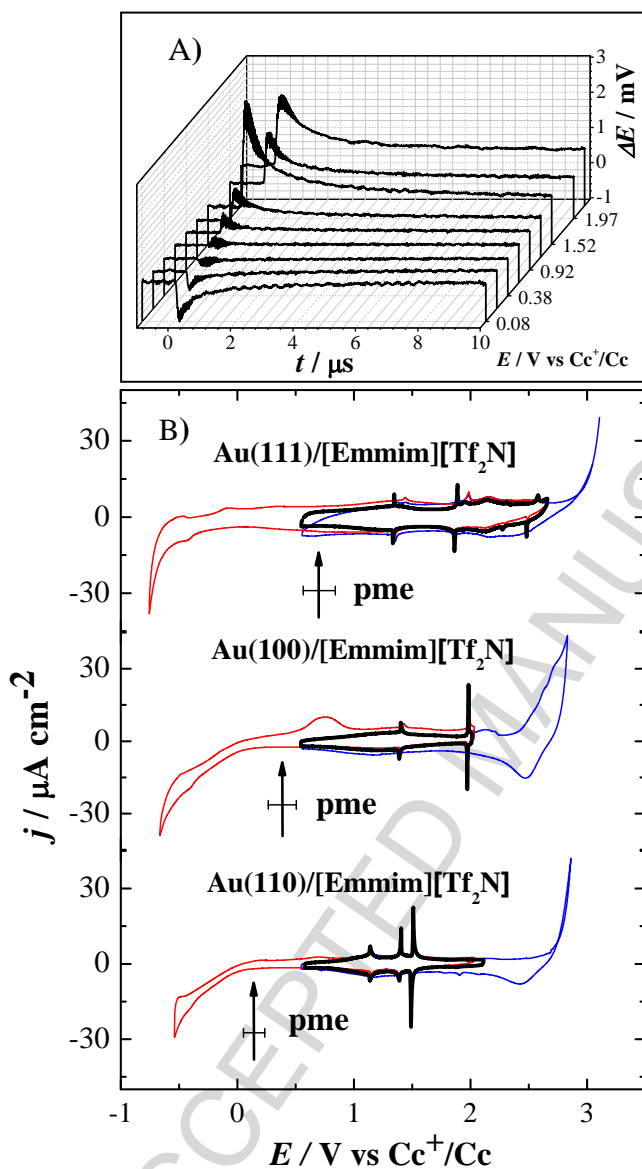
Figure 3: A) Laser-induced coulostatic potential transients measured for a Au(111) in [Emmim][Tf$_2$N], B) Cyclic voltammogram for the different Au basal planes in contact with [Emmim][Tf$_2$N], showing the electrochemical potential window. Potential of maximum entropies for each interface are indicated by arrows. Error bars indicate the uncertainty in the pme determination. Scan rate: 50mV s^{-1}

References.

[1] J.P. Hallett, T. Welton, Room-Temperature Ionic Liquids: Solvents for Synthesis and Catalysis. 2, Chem. Rev., 111 (2011) 3508-3576.
[2] R. Hayes, G.G. Warr, R. Atkin, Structure and Nanostructure in Ionic Liquids, Chem. Rev., 115 (2015) 6357-6426.
[3] M. Armand, F. Endres, D.R. MacFarlane, H. Ohno, B. Scrosati, Ionic-liquid materials for the electrochemical challenges of the future, Nat. Mater., 8 (2009) 621-629.
[4] Y.Z. Su, Y.C. Fu, Y.M. Wei, J.W. Yan, B.W. Mao, The Electrode/Ionic Liquid Interface: Electric Double Layer and Metal Electrodeposition, ChemPhysChem, 11 (2010) 2764-2778.
[5] M. Montiel, J. Solla-Gullón, C. Sánchez-Sánchez, Electrochemical reactivity and stability of platinum nanoparticles in imidazolium-based ionic liquids, J Solid State Electrochem, DOI 10.1007/s10008-015-3014-5.
[6] B.C.M. Martindale, R.G. Compton, Formic acid electro-synthesis from carbon dioxide in a room temperature ionic liquid, Chem. Commun., 48 (2012) 6487-6489.
[7] A.A. Kornyshev, Double-layer in ionic liquids: Paradigm change?, J. Phys. Chem. B, 111 (2007) 5545-5557.
[8] C. Gomes, R. Costa, C.M. Pereira, A.F. Silva, The electrical double layer at the ionic liquid/Au and Pt electrode interface, RSC Adv., 4 (2014) 28914-28921.
[9] Y.-X. Zhong, J.-W. Yan, M.-G. Li, X. Zhang, D.-W. He, B.-W. Mao, Resolving Fine Structures of the Electric Double Layer of Electrochemical Interfaces in Ionic Liquids with an AFM Tip Modification Strategy, J. Am. Chem. Soc., 136 (2014) 14682-14685.
[10] Y.Z. Su, J.W. Yan, M.G. Li, M. Zhang, B.W. Mao, Electric Double Layer of Au(100)/Imidazolium-Based Ionic Liquids Interface: Effect of Cation Size, J. Phys. Chem. C, 117 (2013) 205-212.
[11] K. Motobayashi, K. Minami, N. Nishi, T. Sakka, M. Osawa, Hysteresis of Potential-Dependent Changes in Ion Density and Structure of an Ionic Liquid on a Gold Electrode: In Situ Observation by Surface-Enhanced Infrared Absorption Spectroscopy, J. Phys. Chem. Lett., 4 (2013) 3110-3114.
[12] M. Zhang, L.J. Yu, Y.F. Huang, J.W. Yan, G.K. Liu, D.Y. Wu, Z.Q. Tian, B.W. Mao, Extending the shell-isolated nanoparticle-enhanced Raman spectroscopy approach to interfacial ionic liquids at single crystal electrode surfaces, Chem. Commun., 50 (2014) 14740-14743.
[13] X. Zhang, Y.X. Zhong, J.W. Yan, Y.Z. Su, M. Zhang, B.W. Mao, Probing double layer structures of Au (111)-BMIPF6 ionic liquid interfaces from potential-dependent AFM force curves, Chem. Commun., 48 (2012) 582-584.
[14] R. Costa, C.M. Pereira, A.F. Silva, Structural ordering transitions in ionic liquids mixtures, Electrochem. Commun., 57 (2015) 10-13.
[15] F. Buchner, K. Forster-Tonigold, B. Uhl, D. Alwast, N. Wagner, H. Farkhondeh, A. Gross, R.J. Behm, Toward the Microscopic Identification of Anions and Cations at the Ionic Liquid I Ag(111) Interface: A Combined Experimental and Theoretical Investigation, ACS Nano, 7 (2013) 7773-7784.
[16] B. Uhl, T. Cremer, M. Roos, F. Maier, H.-P. Steinrück, J. Behm, At the ionic liquid|metal interface: structure formation and temperature dependent behavior of an ionic liquid adlayer on Au(111), Phys. Chem. Chem. Phys., 15 (2013) 17295-17302.
[17] Z. Qian, H. Yining, W. Yonglong, Y. Shihai, Y. Tianying, Comparing the differential capacitance of two ionic liquid electrolytes: Effects of specific adsorption, Electrochem. Commun., 38 (2014) 44-46.
[18] B. Uhl, H.H. Huang, D. Alwast, F. Buchner, R.J. Behm, Interaction of ionic liquids with noble metal surfaces: structure formation and stability of OMIM TFSA and EMIM TFSA on Au(111) and Ag(111), Phys. Chem. Chem. Phys., 17 (2015) 23816-23832.
[19] R. Foulston, S. Gangopadhyay, C. Chiutu, P. Moriarty, R.G. Jones, Mono- and multi-layer adsorption of an ionic liquid on Au(110), Phys. Chem. Chem. Phys., 14 (2012) 6054-6066.

[20] R. Atkin, S.Z. El Abedin, R. Hayes, L.H.S. Gasparotto, N. Borisenko, F. Endres, AFM and STM Studies on the Surface Interaction of BMP TFSA and (EMIm TFSA Ionic Liquids with Au(111), J. Phys. Chem. C, 113 (2009) 13266-13272.

[21] V. Climent, B.A. Coles, R.G. Compton, Laser-induced potential transients on a Au(111) single-crystal electrode. Determination of the potential of maximum entropy of double-layer formation, J. Phys. Chem. B, 106 (2002) 5258-5265.

[22] N. García-Aráez, V. Climent, J. Feliu, Potential-Dependent Water Orientation on Pt(111), Pt(100), and Pt(110), As Inferred from Laser-Pulsed Experiments. Electrostatic and Chemical Effects, J. Phys. Chem. C, 113 (2009) 9290-9304.

[23] V. Climent, B.A. Coles, R.G. Compton, Coulostatic potential transients induced by laser heating of a Pt(111) single-crystal electrode in aqueous acid solutions. Rate of hydrogen adsorption and potential of maximum entropy, J. Phys. Chem. B, 106 (2002) 5988-5996.

[24] P. Sebastián, A.P. Sandoval, V. Climent, J.M. Feliu, Study of the interface Pt(111)/ [Emmim][NTf2] using laser-induced temperature jump experiments, Electrochem. Commun., 55 (2015) 39-42.

[25] K. Dong, S.J. Zhang, Hydrogen Bonds: A Structural Insight into Ionic Liquids, Chem.-Eur. J., 18 (2012) 2748-2761.

[26] M. Gnahm, D.M. Kolb, The purification of an ionic liquid, J. Electroanal. Chem., 651 (2011) 250-252.

[27] A.P. Sandoval, M.F. Suárez-Herrera, J.M. Feliu, Hydrogen redox reactions in 1-ethyl-2,3-dimethylimidazolium bis(trifluoromethylsulfonyl)imide on platinum single crystal electrodes, Electrochem. Commun., 46 (2014) 84-86.

[28] M. Gnahm, C. Müller, R. Répánszki, T. Pajkossy, D.M. Kolb, The interface between Au(100) and 1-butyl-3-methyl-imidazolium-hexafluorophosphate Phys. Chem. Chem. Phys., 13 (2011) 11627-11633.

[29] C. Müller, S. Vesztergom, T. Pajkossy, T. Jacob, The interface between Au(100) and 1-butyl-3-methyl-imidazolium-bis(trifluoromethylsulfonyl)imide, J. Electroanal. Chem., 737 (2015) 218-225.

[30] M.J.A. Shiddiky, A.A.J. Torriero, C. Zhao, I. Burgar, G. Kennedy, A.M. Bond, Nonadditivity of Faradaic Currents and Modification of Capacitance Currents in the Voltammetry of Mixtures of Ferrocene and the Cobaltocenium Cation in Protic and Aprotic Ionic Liquids, J. Am. Chem. Soc., 131 (2009) 7976-7989.

[31] T. Dretschkow, T. Wandlowski, Structural transitions in organic adlayers - a molecular view, in Solid Liquid Interface Properties and Processes – A Surface Science Approach, K. Wandelt (Ed.) Springer-Verlag, 2003.

[32] J. Lipkowski, Z.C. Shi, A.C. Chen, B. Pettinger, C. Bilger, Ionic adsorption at the Au(111) electrode, Electrochim. Acta, 43 (1998) 2875-2888.

[33] J. Clavilier, The role of anion on the electrochemical behaviour of a {111} platinum surface; an unusual splitting of the voltammogram in the hydrogen region, J.Electroanal.Chem., 107 (1979) 211-216.

[34] J.M. Feliu, M.J. Valls, A. Aldaz, M.A. Climent, J. Clavilier, Alkali metal cations and pH effects on a splitting of the unusual adsorption states of Pt(111) voltammograms in phosphate buffered solutions, J. Electroanal. Chem., 345 (1993) 475-481.

[35] D.M. Kolb, Reconstruction phenomena at metal-electrolyte interfaces, Prog. Surf. Sci., 51 (1996) 109-173.

[36] G. Feng, X.K. Jiang, R. Qiao, A.A. Kornyshev, Water in Ionic Liquids at Electrified Interfaces: The Anatomy of Electrosorption, ACS Nano, 8 (2014) 11685-11694.

[37] A. Uysal, H. Zhou, G. Feng, S.S. Lee, S. Li, P. Fenter, P.T. Cummings, P.F. Fulvio, S. Dai, J.K. McDonough, Y. Gogotsi, Structural Origins of Potential Dependent Hysteresis at the Electrified Graphene/Ionic Liquid Interface, J. Phys. Chem. C, 118 (2014) 569-574.

[38] J. Lecoeur, J. Andro, R. Parsons, the behavior of water at stepped surfaces of single-crystal gold electrodes, Surf. Sci., 114 (1982) 320-330.

Highlights

The interphase between Au(hkl) and the ionic liquid [Emmim][Tf2N] is investigated.

The voltammetric profile contains sharp peaks corresponding to phase transitions.

These sharp peaks are very sensitive to the crystallographic structure.

Laser induce temperature jump is used to determine the potential of maximum entropy.

12